Co-published by
Institute of Fluid-Flow Machinery
Polish Academy of Sciences
Committee on Thermodynamics and Combustion
Polish Academy of Sciences

http://www.imp.gda.pl/archives-of-thermodynamics/

Impact of finite Larmor radius on the onset of Rayleigh-Taylor instability of stratified magnetised Jeffrey plasma fluid

Anukampa Thakur[a], Veena Sharma[a], Gian Chand Rana[b*], Poonam Gautam[c]

[a]Department of Mathematics and Statistics, Himachal Pradesh University, Summer Hill, Shimla 171005, India
[b]Principal, Govrenment Degree College Dhaneta, Hamirpur, Himachal Pradesh 177041, India
[c]School of Basic Sciences, Bahra University, Waknaghat, Solan, Himachal Pradesh 173234, India
*Corresponding author email: drgcrana15@gmail.com

Received: 19.03.2025; revised: 09.08.2025; accepted: 12.08.2025

Abstract

This study explores the stabilising interplay of finite Larmor radius corrections and quantum pressure on the Rayleigh-Taylor instability in a non-Newtonian, magnetised fluid. The investigation is motivated by the need to understand how quantum and magnetohydrodynamic effects jointly influence instability behaviour in complex fluid systems. The governing magnetohydrodynamic equations are linearised using normal mode analysis and appropriate boundary conditions to derive a general dispersion relation for Rayleigh-Taylor instability under the Jeffrey fluid model. Numerical results show that the combined presence of finite Larmor radius corrections and quantum pressure suppresses the growth rate of Rayleigh-Taylor instability modes. In contrast, the Jeffrey parameter amplifies instability, while quantum and finite Larmor radius effects reduce both the cut-off and critical wavenumbers.

Keywords: Rayleigh-Taylor instability; Jeffrey model; Finite Larmor radius; Magnetic field; Quantum pressure

Vol. 46(2025), No. 4, 95–103; doi: 10.24425/ather.2025.156840

Cite this manuscript as: Thakur, A., Sharma, V., Rana, G.C., & Gautam, P. (2025). Impact of finite Larmor radius on the onset of Rayleigh-Taylor instability of stratified magnetised Jeffrey plasma fluid. *Archives of Thermodynamics*, 46(4), 95–103.

1. Introduction

The Rayleigh-Taylor instability (RTI) arises at the interface between fluids of differing densities when a heavier fluid is placed above a lighter one in the presence of a vertical gravitational field [1]. This type of instability plays a crucial role in various physical and astrophysical phenomena, including laser–plasma interactions, Z-pinch implosions and magnetised target fusion, as well as in systems such as inertial confinement fusion, galaxy clusters and dense plasma focus devices. Goldston and Rutherford [2] extended the analysis of RTI to fluids with continuously varying density profiles and demonstrated that angular velocity, mass concentration and stress relaxation time have a stabilising influence on the instability.

The significant potential of quantum plasma in diverse fields − such as laser fusion, white dwarfs, semiconductor devices and dense astrophysical plasmas − has recently drawn extensive research interest. Quantum plasma consists of charged particles exhibiting distinct behaviour at moderate temperatures, differing from classical plasmas. This quantum effect arises when the de Broglie wavelength of charged particles becomes comparable to or larger than the system's characteristic length [3]. The pressure term in the equations of motion is divided into two terms, $p = p^C + p^Q$ (p^C – classical pressure, p^Q – quantum pressure), by using Wingen principle and Schrödinger wave equation in the momentum equations, $(-\nabla p)$ and $\boldsymbol{Q} = \frac{\hat{h}^2}{2m_e m_i}\rho\nabla\left(\frac{\nabla^2\sqrt{\rho}}{\sqrt{\rho}}\right)$. A lot of work has been done in this direction to evaluate the growth rates of RTI in various processes with quantum pressure by many researchers, both theoretically and experimentally.

Gardner [4] noticed that the quantum hydrodynamic conservation laws have the same form as the classical hydrodynamic

Nomenclature

d – thickness of layer, m
e_{ij} – rate of strain tensor
g – gravitational acceleration, m/s^2
$\hat{h}$ – Planck constant, 6.62607015×10^{-34} m^2 kg/s
H – magnetic field, A/m
k – wave number, 1/m
k_{max} – cut-off wave number, 1/m
L_D – length scale, m
m_e – mass of electron, amu
m_i – mass of ion, amu
n – growth rate, 1/s
n_i – growth rate of RTI, 1/s
n_q – quantum parameter, kg m/s
p – pressure, Pa
p^C – classical pressure, Pa
p^Q – quantum pressure, Pa
$\boldsymbol{Q}$ – quantum pressure, Pa
t – time, s
T – temperature, K
T_{ij} – stress tensor, Pa
$\boldsymbol{u}$ – velocity vector of fluid, m/s
u_j – velocity vector components, m/s
u, v, w – velocity vector components, m/s
x, y, z – Cartesian coordinates, m

Greek symbols

δ_{ij} – Kronecker delta
λ – Jeffrey parameter
λ_0 – stress relaxation time parameter
λ_1 – strain retardation time parameter
μ – dynamic viscosity, Pa·s
μ_e – magnetic permeability, H/m
ν – kinematic viscosity, m^2/s
ν_{FR} – finite Larmor radius correction, kg/(m^2 s^2)
ρ – density, kg/m^3
τ_{ij} – viscous stress tensor
Ω – ion gyro-frequency, rad/s

Abbreviations and Acronyms

FLR – finite Larmor radius
ICF – inertial confinement fusion
MHD – magnetohydrodynamics
QMHD – quantum magnetohydrodynamics
RTI – Rayleigh-Taylor instability

equations. Haas [5] employed the quantum hydrodynamics model to analyse charge mobility in dense quantum plasmas. Elena et al. [6] investigated the influence of quantum effects on RTI and internal waves in plasmas, while Bychkov et al. [7] studied RTI in incompressible, stratified quantum plasmas, establishing that quantum pressure at low temperatures stabilises perturbation growth. Sharma et al. [8] explored the combined effects of angular velocity and surface tension on the stability of two superimposed fluids embedded with dust particles. Hoshoudy [9−11], and Hoshoudy and Awasthi [12] analysed RTI in stratified quantum plasmas under the influence of vertical magnetic fields and viscosity, concluding that quantum pressure, in conjunction with the magnetic field, plays a crucial role in stabilising the system and suppressing RTI. Additionally, Hoshoudy and Prajapati [13] demonstrated the impact of suspended particles on RTI, observing a stabilising effect due to both quantum pressure and dust particle mass concentration.

Sharma and Gupta [14] examined the stability of an elastico-viscous fluid under the influence of magnetic field and rotation. Dolai and Prajapati [15] analysed RTI in strongly coupled, dusty, rotating plasmas and observed significant suppression of instability due to the combined influence of shear and angular velocities. Micro-level instabilities in plasmas are often described by models incorporating collisionless dissipative effects, finite Larmor radius (FLR) corrections and other non-ideal behaviours. Although the length and time scales associated with micro-instabilities typically match those of transport coefficients and turbulence – leading to a common practice of neglecting FLR effects – this assumption breaks down when the Larmor radius becomes comparable to the hydromagnetic wavelength or when the ion gyrofrequency approaches the wave frequency. Under such conditions, the FLR must be considered. Consequently, the time and spatial scales at which magnetohydrodynamics (MHD) fails align with the scales of ion gyration and the ion Larmor frequency.

The effects of finite Larmor radius have drawn significant attention due to their applicability in a range of astrophysical environments, including mirror machines, the solar corona, and both interplanetary and interstellar plasmas, particularly in the presence of gyro-viscous forces. Rosenbluth et al. [16] demonstrated the stabilising influence of FLR on RTI by employing plasma fluid equations. Roberts and Taylor [17] extended MHD theory by incorporating finite Larmor radius effects. Jukes [18] showed that FLR can suppress RTI, though with some constraints introduced by the presence of a sheared magnetic field. Following these foundational studies, numerous investigations explored the effects of FLR, dust particles, rotation and viscosity on RTI in continuously stratified magnetofluids [19−22]. Notably, Tiwari et al. [23] were the first to establish the influence of FLR corrections on the RTI in an inviscid, stratified plasma, incorporating both magnetic fields and quantum pressure. They concluded that FLR corrections suppress the instability more effectively than quantum pressure alone. Sun et al. [24] highlighted the RTI in magnetised fluids relevant to inertial confinement fusion (ICF), emphasising that viscosity, rather than electrical resistivity, plays a dominant role in determining the interface dynamics.

It is important to note that most of the aforementioned studies have been conducted in the context of Newtonian plasma fluids. However, in recent years, the mechanisms and applications of non-Newtonian fluids described by various rheological models have gained considerable interest due to their relevance in both industrial (e.g. chemical processing) and astrophysical settings. A fluid is characterised as Newtonian or non-Newtonian based on the nature of the relationship between stress and strain rate, expressed through its constitutive equation. Among non-Newtonian models, the Jeffrey fluid model [25] is of particular interest in this study. It exhibits linear viscoelastic behaviour, yield stress, shear-thinning properties and high shear viscosity,

making it well-suited for modelling complex plasma dynamics with non-Newtonian characteristics.

In Jeffrey fluid, the two-time parameters – namely, the strain retardation time and stress relaxation time – play a significant role in understanding wave propagation phenomena, such as those occurring within the Earth's mantle. The strain retardation time relates to the delay in deformation under stress, while the stress relaxation time represents the time a fluid takes to return from a disturbed state to its original equilibrium. Fluids exhibiting such time-dependent behaviour are particularly relevant in environmental and biomedical applications, including polypropylene coalescence sintering, geological flows and blood flow dynamics.

Yadav [26–28] investigated the effects of anisotropy, electric fields, and thermal non-equilibrium on the onset and instability mechanisms of Jeffrey fluid convection in various porous media configurations and found that rotation and anisotropy in thermal diffusivity delay the onset of Jeffrey fluid convection, whereas the Jeffrey parameter and permeability anisotropy exhibit dual effects under rotation. Increased electric field and internal heating parameters reduce system stability. Gautam et al. [29] investigated the influence of an electric field on thermal convection in a nanofluid-saturated porous medium, whereas Sharma et al. [30] analysed the Rayleigh-Taylor instability of superposed dusty Jeffrey fluids in a porous medium, considering interfacial surface tension. Yadav et al. [31–32] analysed the Horton-Rogers-Lapwood problem and convective flow of ethylene glycol-silver Jeffrey nanofluid in a Hele-Shaw cell under the influence of a magnetic field.

Prajapati [33] investigated RTI in a strongly coupled viscoelastic fluid, considering the effects of non-homogeneous magnetic fields, uniform rotation and density gradients, and observed a substantial suppression of the instability. Garai et al. [34] examined RTI in viscoelastic plasma embedded with dust particles and magnetic fields, highlighting the significant stabilising influence of non-Newtonian properties. Dey [35] explored Jeffrey fluid flow in the presence of suspended particles and angular velocity, including the Hall effect and volume fraction, and concluded that non-Newtonian parameters tend to have a retarding influence on the evolution of instability in the system. Garai et al. [36] analysed RTI in strongly coupled quantum plasma with shear velocity and found that shear effects could either suppress or trigger instability, depending on the direction of the shear velocity gradient. Adak et al. [37] studied RTI in inhomogeneous pair-ion plasma and derived the instability criteria for the classical case.

Das et al. [38] investigated the collective behaviour of strongly coupled dusty plasma, whereas Dharodi and Das [39] performed numerical simulations on gravity-driven instabilities in such plasmas. The result indicates that increasing the coupling strength of the medium leads to suppression of these instabilities. Dharodi [40–41] conducted numerical investigations on gravity-driven instabilities in strongly coupled dusty plasmas, focusing on hetero-interactions between a rising bubble and a falling droplet, as well as homo-interactions between pairs of rising or falling bubbles/droplets. The study revealed that, under gravity, the formation of counter-rotating vorticity lobes causes bubbles to ascend and droplets to descend. In viscoelastic fluids, besides the initial separation, shear waves generated by rotating vortices were found to play a key role in bringing two droplets or bubbles closer together.

Motivated by the work presented above, this study focuses on investigating the influence of FLR corrections on the Rayleigh-Taylor instability in a non-Newtonian plasma fluid arranged in horizontal stratification, incorporating quantum pressure effects. The RTI is a fundamental plasma instability that plays a critical role in astrophysical plasmas, ICF and space weather phenomena. Understanding the onset and control of RTI under the influence of quantum and magnetic effects is crucial for enhancing the stability of fusion plasmas and improving performance in high-energy density systems. The inclusion of FLR corrections and non-Newtonian (Jeffrey) fluid behaviour provides a more realistic model for magnetised plasmas found in laboratory and astrophysical environments, such as solar prominences, planetary magnetospheres and accretion disks. The novelty of this study lies in the combined consideration of quantum pressure effects, FLR corrections and non-Newtonian fluid dynamics (via the Jeffrey model) in analysing RTI. While previous studies have independently examined RTI in Newtonian or classical fluids with either quantum effects or magnetic field influences, this is the first comprehensive analysis that integrates all three aspects simultaneously in a stratified magnetised plasma system. Moreover, the use of the Jeffrey fluid model introduces a new viscoelastic framework that captures memory effects absent in earlier studies. The non-Newtonian behaviour of the plasma is modelled using the Jeffrey fluid framework, which effectively captures viscoelastic features and complex rheological behaviour.

2. Mathematical models

The equation that governs the behaviour of fluid flow in the context of Jeffrey fluid, as formulated by [26-32], can be expressed as follows:

$$T_{ij} = -p\delta_{ij} + \tau_{ij} \tag{1}$$

and

$$\tau_{ij} = -p\delta_{ij} + \frac{2\mu}{1+\lambda}\left[1 + \lambda_1\left\{\frac{\partial(2e_{ij})}{\partial t} + \frac{\partial u_i}{\partial x_j}\right\}\right]e_{ij}. \tag{2}$$

For incompressible fluids, the above relation reduces to

$$\tau_{ij} = -p\delta_{ij} + \frac{2\mu}{1+\lambda}e_{ij}. \tag{3}$$

Here, an incompressible, heterogeneous, infinitely extending and infinitely electrically conducting viscoelastic Jeffrey fluid of finite thickness d, comprised of the planes $z = 0$ and $z = d$, is organised in a horizontal layer of electrons and immobile ions saturating homogeneous, isotropic porous media. A uniform gravitational field $\boldsymbol{g}(0,0,-g)$ acts vertically downward, thereby influencing the buoyancy-driven motion within the system. In addition, the plasma is subjected to a uniform externally applied magnetic field $\boldsymbol{H}(H,0,0)$ directed along the horizontal axis, introducing magnetohydrodynamic (MHD) effects into the flow. The presence of a quantum pressure term $\boldsymbol{Q}$, originating from quantum mechanical effects associated with electron degeneracy, further modifies the momentum balance and contributes to

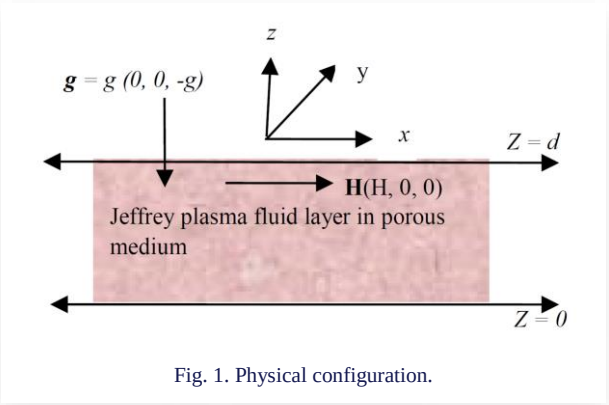

Fig. 1. Physical configuration.

stabilising or destabilising tendencies in the convective motion. The schematic representation of the physical system, along with the associated external forces and boundary constraints, is illustrated in Fig. 1.

The equations of momentum balance in quantum hydrodynamics (QHD) are [33–37]:

$$\rho\left[\frac{\partial}{\partial t}+\boldsymbol{u}\cdot\nabla\right]\boldsymbol{u}=-\nabla p+\rho\boldsymbol{g}+\nabla\cdot\mathbf{P}+\boldsymbol{Q}+\frac{\mu}{1+\lambda}\nabla^2\boldsymbol{u}+ +\frac{\mu_e}{4\pi}(\nabla\times\boldsymbol{H})\times\boldsymbol{H}, \tag{4}$$

where $\boldsymbol{u}, \rho, p, \mu, \lambda$, and μ_e represent the velocity of fluid, density, pressure, dynamic viscosity, Jeffrey parameter and magnetic permeability, respectively. Here, **P** represents the pressure tensor that anticipates the finite Larmor radius effects.

The mass balance equation of incompressible plasma fluid is

$$\nabla\cdot\boldsymbol{u}=0. \tag{5}$$

The condition of compressibility implies that the fluid density is not constant and may vary with pressure and temperature. Accordingly, the continuity equation takes the general form as:

$$\frac{\partial\rho}{\partial t}+(\boldsymbol{u}\cdot\nabla)\rho=0. \tag{6}$$

In various circumstances of physical intrigue in ICF, instability occurs at velocities much smaller than that of local sound speed. Consequently, accelerations in flow are too weak to vary the fluid flow density appreciably, and the fluid moves without expanding or compressing, meaning that elements of fluid move with constant density, as seen in Eq. (6).

Maxwell's equations, due to the presence of a magnetic field, are:

$$\nabla\cdot\boldsymbol{H}=0, \tag{7}$$

$$\frac{\partial\boldsymbol{H}}{\partial t}=\nabla\times(\boldsymbol{u}\times\boldsymbol{H}). \tag{8}$$

Furthermore, the initial steady state is characterised by no flow motion and each physical variable varies along the vertical, i.e. z-axis, only. Therefore, the steady state solutions are given as

$$\boldsymbol{u}=(0,0,0),\quad p=p(z),\quad \rho=\rho(z),\quad \boldsymbol{Q}=\boldsymbol{Q}(z). \tag{9}$$

To investigate the stability of the hydrodynamic motion, infinitesimal perturbations are superimposed on each of the physical quantities of the initial state solutions as

$$\begin{gathered}\rho=\rho_0+\rho',\quad p=p_0+p',\quad \boldsymbol{H}=\boldsymbol{H}_0+\boldsymbol{h},\\ \boldsymbol{u}=\boldsymbol{u}_0+\boldsymbol{u}',\quad \boldsymbol{Q}=\boldsymbol{Q}_0+\boldsymbol{Q}',\end{gathered} \tag{10}$$

where $p',\ \rho',\ \boldsymbol{h}(h_x,h_y,h_z),\ \boldsymbol{u}'(u,v,w),\ \boldsymbol{Q}'(Q_{x1},Q_{y1},Q_{z1})$ represent the perturbations in the pressure, the density of fluid, the magnetic field, the plasma fluid velocity and the quantum force, respectively. The subscript '0' denotes the equilibrium state.

Utilising the disturbance equations (10) and the linear theory, Eqs. (4)−(8) take linear form as

$$\nabla\cdot\boldsymbol{u}'=0, \tag{11}$$

$$\rho\frac{\partial\boldsymbol{u}'}{\partial t}=-\nabla p'+\boldsymbol{g}\rho'-\nabla\cdot\mathbf{P}+\boldsymbol{Q}'+\frac{\mu}{1+\lambda}\nabla^2\boldsymbol{u}' +\frac{\mu_e}{4\pi}[(\nabla\times\boldsymbol{h})\times\boldsymbol{H}], \tag{12}$$

$$\frac{\partial\rho'}{\partial t}+(\boldsymbol{u}\cdot\nabla)\rho=0, \tag{13}$$

$$\nabla\cdot\boldsymbol{h}=0, \tag{14}$$

$$\frac{\partial\boldsymbol{h}}{\partial t}=\nabla\times(\boldsymbol{u}\times\boldsymbol{H}), \tag{15}$$

where

$$\boldsymbol{Q}'=\frac{\hat{h}^2}{2m_em_i}\left[\begin{array}{l}\frac{1}{2}\nabla(\nabla^2\rho')-\frac{1}{2\rho}\nabla\rho'\nabla^2\rho-\frac{1}{2\rho}\nabla\rho\nabla^2\rho'\\ +\frac{\rho'}{2\rho^2}\nabla\rho\nabla^2\rho-\frac{1}{2\rho}\nabla(\nabla\rho\nabla\rho')\\ +\frac{\rho'}{4\rho^2}\nabla(\nabla\rho)^2+\frac{1}{2\rho^2}(\nabla\rho)^2\nabla\rho'\\ +\frac{1}{\rho^2}(\nabla\rho\nabla\rho')\nabla\rho-\frac{\rho'}{\rho^3}(\nabla\rho)^3\end{array}\right]. \tag{16}$$

For the horizontal magnetic field, the stress tensor in the component form is [23]:

$$\begin{gathered}P_{xx}=0,\ P_{yy}=-\rho\nu_{FR}\left(\frac{\partial w}{\partial y}+\frac{\partial v}{\partial x}\right),\ P_{zz}=\rho\nu_{FR}\left(\frac{\partial w}{\partial y}+\frac{\partial v}{\partial x}\right),\\ P_{xy}=P_{yx}=-2\rho\nu_{FR}\left(\frac{\partial u}{\partial z}\right),\ P_{xz}=P_{zx}=2\rho\nu_{FR}\left(\frac{\partial u}{\partial y}\right),\\ P_{yz}=P_{zy}=\rho\nu_{FR}\left(\frac{\partial v}{\partial y}-\frac{\partial w}{\partial x}\right),\end{gathered} \tag{17}$$

where $\nu_{FR}=\frac{a^2\Omega}{4}$ represents the FLR correction, with *a* being the ion Larmor radius and Ω denoting the ion gyrofrequency.

3. Methodology adopted

To investigate the stability of a system, perturbations in physical variables are analysed in terms of modes by ascribing a horizontal wave number, depending on *y*, *z* and time (*t*), are supposed to vary as

$$f'(y,z,t)=f(z)\exp[i(ky+nt)], \tag{18}$$

where *i* is the imaginary unit, and the term $\exp[i(ky+nt)]$ represents a **wave-like disturbance** varying sinusoidally in space

(in the *y*-direction with the wave number *k*) and in time (with the growth rate *n*).

Using Eq. (18), Eqs. (11)–(15) transform to Cartesian components as:

$$ikv + Dw = 0, \tag{19}$$

$$\rho inv = -ikp' + \rho\nu_{FR}(D^2 - k^2)w + 2\nu_{FR}D\rho Dw + \frac{\mu}{1+\lambda}(D^2 - k^2)v + Q_{y1}, \tag{20}$$

$$\rho inw = -Dp' - g\rho' - \nu_{FR}D\rho(ikw + Dw) - \rho\nu_{FR}(D^2 - k^2)v + \frac{\mu}{1+\lambda}(D^2 - k^2)w + Q_{z1}, \tag{21}$$

$$in\rho' + wD\rho = 0, \tag{22}$$

$$h_x = h_y = h_z = 0, \tag{23}$$

where

$$Q_{y1} = \frac{k_y}{k_x}\frac{\hat{\hbar}^2}{2\varepsilon n m_e m_i}\left[\begin{array}{c} \frac{1}{2}D\rho D^2 w + \left\{D^2\rho - \frac{1}{2\rho}(D^2\rho)^2\right\}Dw + \\ \left\{\frac{1}{2}D^3\rho - \frac{1}{\rho}D\rho D^2\rho - \frac{k^2}{2}D\rho + \frac{1}{2\rho^2}(D\rho)^3\right\}w \end{array}\right], \tag{24}$$

$$Q_{z1} = \frac{\hat{\hbar}^2}{2\varepsilon n m_e m_i}\left[\begin{array}{c} \frac{1}{2}D\rho D^3 w + \left\{\frac{3}{2}D^2\rho - \frac{1}{\rho}(D^2\rho)^2\right\}D^2 w + \\ \left\{\frac{1}{2}D^3\rho - \frac{1}{\rho}D\rho D^2\rho - \frac{k^2}{2}D\rho + \frac{3}{2\rho^2}(D\rho)^3\right\}Dwk^2 \\ + \frac{1}{2}D^4\rho - \frac{1}{\rho}D\rho D^3\rho - \frac{k^2}{2}D^2\rho - \frac{1}{\rho}(D^2\rho)^2 \\ + \frac{5}{2\rho^2}(D\rho)^2 D^2\rho + \frac{k^2}{2\rho}(D\rho)^2 - \frac{1}{\rho}(D\rho)^4 \end{array}\right]. \tag{25}$$

In the above, *D* stands for $\frac{d}{dz}$, ε is the medium porosity, and k_x and k_y are the horizontal and vertical components of the wave number, respectively.

On eliminating v, ρ', and p' from Eq. (17) and using Eqs. (15)–(16) and Eqs. (18)–(21), we get the general differential equation for w as

$$\left[\rho n^2 + 2\nu_{FR}knD\rho + \frac{\mu kn}{1+\lambda}D\rho + k^2A\right]D^2 w + [n^2 D\rho + 2\nu_{FR}knD^2\rho + k^2 B]Dw - \left[\rho n^2 k^2 + \left(2\nu_{FR}kn + \frac{\mu kn}{1+\lambda} + g - C\right)k^2 D\rho\right]w = 0. \tag{26}$$

Here

$$A = -\frac{\hat{\hbar}^2}{4m_e m_i}\frac{1}{\rho}(D\rho)^2, B = -\frac{\hat{\hbar}^2}{4m_e m_i}\frac{1}{\rho}D\rho[(D\rho)^2 - 2\rho D^2\rho], \quad C = -\frac{\hat{\hbar}^2}{4m_e m_i}\frac{k^2}{\rho}D\rho.$$

The density of fluid is assumed to vary exponentially with respect to *z* and depends on L_D– a length scale. Thus, the density distribution at $z = 0$ is described as

$$\rho(z) = \rho\exp\left(\frac{z}{L_D}\right). \tag{27}$$

Equation (26), using Eq. (23), after algebraic simplification yields

$$\left[n^2 + \frac{2\nu_{FR}kn}{L_D} + \frac{vkn}{(1+\lambda)L_D} - n_q^2k^2\right]D^2 w + \left[n^2 + \frac{2\nu_{FR}kn}{L_D} + \frac{vkn}{(1+\lambda)L_D} - n_q^2k^2\right]Dw - k^2\left[n^2 + \frac{2\nu_{FR}kn}{L_D} + \frac{vkn}{(1+\lambda)L_D} + \frac{g}{L_D} - n_q^2k^2\right]w = 0, \tag{28}$$

where $\nu = \frac{\mu}{\rho}$ and $n_q^2 = \frac{\hat{\hbar}^2k^2}{2\varepsilon n m_e m_i}$ represent the kinematic viscosity and the quantum parameter accounting for quantum pressure.

The plasma fluid velocity diminishes at $z = 0$ and $z = d$, irrespective of the nature of the bounding surface. Therefore, the solution of Eq. (24) is taken as

$$w = w_1\sin\left(\frac{m_1\pi}{d}z\right)\exp(\lambda z), \tag{29}$$

where m_1 is a positive integer, $\lambda = \frac{1}{2L_D}$ and w_1 is constant.

Using the solutions given in Eq. (29), Eq. (28) gives

$$n^2 + \left(\frac{2\nu_{FR}k}{L_D} + \frac{vk}{(1+\lambda)L_D}\right)n - n_q^2k^2 + \frac{4gk^2d^2L_D}{d^2+4m_1^2\pi^2L_D^2+4m_1^2k^2L_D^2} = 0. \tag{30}$$

Now introducing the non-dimensional variables

$$n^* = \frac{n_1}{n_{pe}},\ n_q^{*2} = \frac{\hat{\hbar}^2}{4m_e m_i L_D^4 n_{pe}^2},\ \nu^* = \frac{\nu}{L_D^2 n_{pe}^2},\ \nu_{FR} = \frac{\nu_{FR}}{L_D^2 n_{pe}^2},\ d^{*2} = \frac{d^2}{L_D^2},\ k^{*2} = k^2L_D^2,\ g^* = \frac{g}{n_{pe}L_D}. \tag{31}$$

Equation (30) (the asterisks are omitted for the sake of convenience) transforms to

$$n^2 + \left(2\nu_{FR}k + \frac{vk}{1+\lambda}\right)n - n_q^2k^2 + \frac{4gk^2d^2}{d^2+4m_1^2\pi^2+4d^2k^2} = 0. \tag{32}$$

It is noteworthy from Eq. (32) that stability/instability of the Rayleigh-Taylor configuration is modified in the presence of FLR corrections, quantum pressure and Jeffrey parameter. Also, it is observed that RTI remains uninfluenced due to the presence of the magnetic field.

Substituting $n = n_r + in_i$ (n_r and n_i are real numbers) in Eq. (32) and separating real and imaginary parts, we get

$$(n_r^2 - n_i^2) - \left(2\nu_{FR}k + \frac{vk}{1+\lambda}\right)n_i - n_q^2k^2 + \frac{4gk^2d^2}{d^2+4m_1^2\pi^2+4d^2k^2} = 0 \tag{33}$$

and

$$2n_r n_i + \left(2\nu_{FR}k + \frac{vk}{1+\lambda}\right)n_r = 0,$$

which implies that $n_r = 0$.

Putting $n_r = 0$ in Eq. (32), one gets

$$n_i^2 + \left(2\nu_{FR}k + \frac{vk}{1+\lambda}\right)n_i + n_q^2k^2 - \frac{4gk^2d^2}{d^2+4m_1^2\pi^2+4d^2k^2} = 0, \tag{34}$$

which is the required relation between *n* and *k* to examine the Rayleigh-Taylor instability in a stratified non-Newtonian plasma

fluid with FLR corrections, quantum pressure and Jeffrey parameter.

3.1. Special cases

For non-viscous Newtonian fluid, i.e. $\nu = 0,\ \lambda = 0$, Eq. (34) condenses to

$$n_i^2 + 2\nu_{FR}kn_i + n_q^2k^2 - \frac{4gk^2d^2}{d^2+4m_1^2\pi^2+4d^2k^2} = 0, \qquad (35)$$

which coincides with the earlier result of Tiwari et al. [23].

4. Numerical results and discussion

To investigate the influence of the Jeffrey parameter, FLR and quantum pressure on both classical and non-classical cases of stratified RTI, the growth rate frequency of the most unstable mode has been numerically computed from the dispersion relation given in Eq. (29), using Mathematica (version 12). The permissible experimental values of all the involved parameters used by Tiwari et al. [23] and Dey [35], and many others, are taken as $\nu_{FR} = 0.5, n_q = 0.6, \lambda = 0.3, m_1 = 1, d = 1$ and $g = 10$, respectively. The growth rate (n_i) of RTI against wave number (k) is plotted to analyse the effect of distinct values of FLR correction, $\nu_{FR} = 0.3, 0.5, 0.9$ in Figs. 2 and 3 for both classical and quantum cases, respectively. The plots in Figs. 2 and 3 clearly show that increasing the FLR correction parameter leads to a notable reduction in the growth rate of RTI in a stratified plasma fluid. This suppression weakens the formation of Rayleigh-Taylor structures and significantly dampens the instability dynamics, particularly in dense plasma systems. Thus, the FLR correction plays a stabilising role by effectively mitigating RTI in both classical and non-classical regimes. Additionally, it is observed that the cut-off wave number k_{max} corresponding to the maximum growth rate shifts to lower values under the influence of quantum pressure, further contributing to the suppression of the instability.

Figures 4 and 5 illustrate the impact of distinct values of the non-dimensional quantum parameter accounting for quantum pressure, n_q = 0.3, 0.5, 0.7, on the growth rate of RTI versus wave number, with and without FLR corrections, respectively. The curves indicate a decrease in the frequency and growth rate of RTI with increasing quantum pressure. Consequently, both

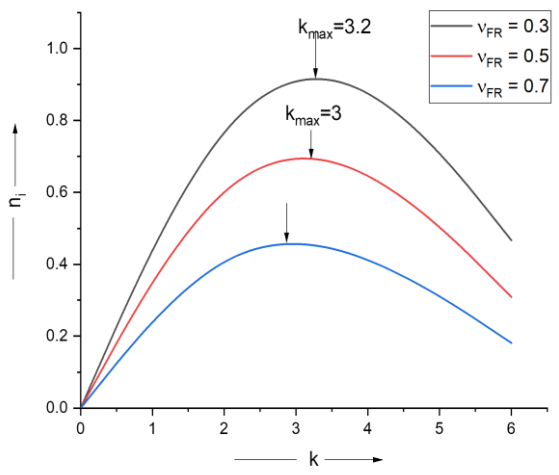

Fig. 2. Impact of FLR correction (ν_{FR}) on the growth rate of RTI (n_i) against the wave number (k), with quantum pressure.

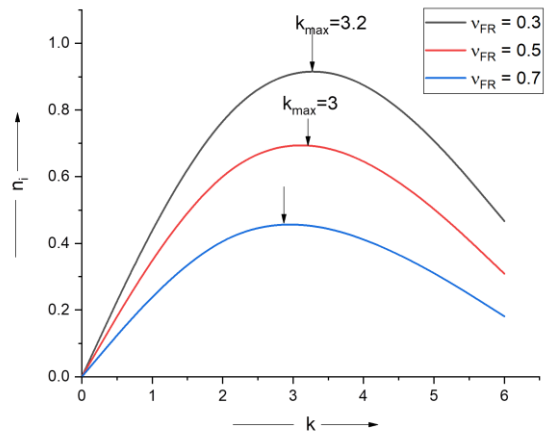

Fig. 3. Impact of FLR correction (ν_{FR}) on the growth rate of RTI (n_i) against the wave number (k), with no quantum pressure.

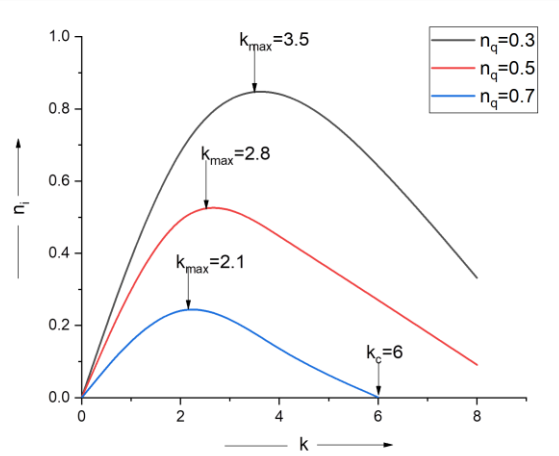

Fig. 4. Impact of the quantum pressure on the growth rate of RTI (n_i) against the wave number (k), with FLR correction.

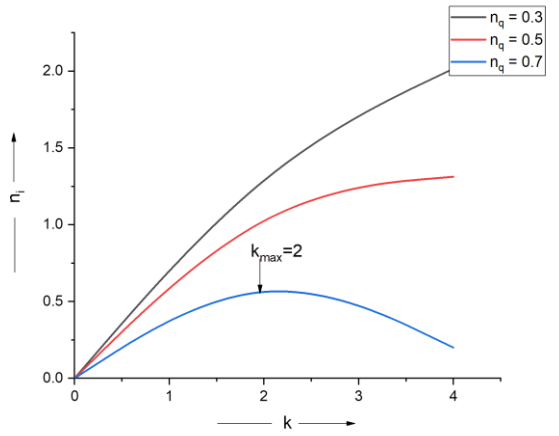

Fig. 5. Impact of the quantum pressure on the growth rate of RTI (n_i) against the wave number (k), with no FLR correction.

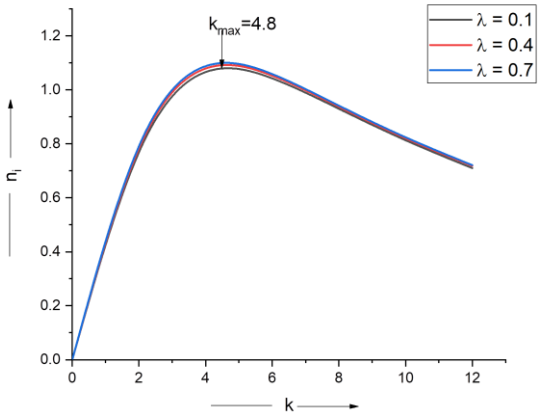

Fig. 6. Impact of the Jeffrey parameter (λ) on the growth rate of RTI (n_i) against the wave number (k), with no quantum pressure (classical case).

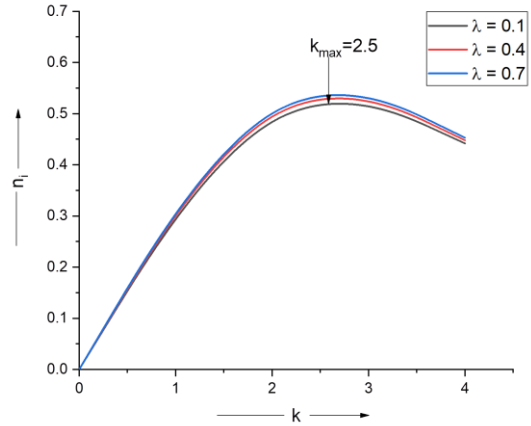

Fig. 7. Impact of the Jeffrey parameter (λ) on the growth rate of RTI (n_i) against the wave number (k), with quantum pressure.

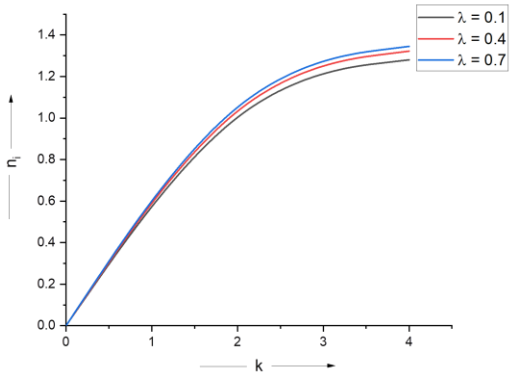

Fig. 8. Impact of the Jeffrey parameter on the growth rate (n_i) of RTI against the wave number (k), with quantum pressure and no FLR corrections.

quantum pressure and FLR corrections demonstrate a stabilising influence by effectively suppressing the growth of instability in non-Newtonian stratified plasma fluids. It is noticed from Fig. 3 that the growth rate starts to decrease for $k > k_{max}$ and complete stability occurs at $k_c = 6.0$ in lieu of both quantum pressure and FLR corrections.

In Figs. 6 and 7, the influence of various values of the Jeffrey parameter, $\lambda = 0.1, 0.4, 07$, on the growth rate of Rayleigh-Taylor instability for both quantum and classical cases, is displayed. The curves illustrate that the growth rate of RTI increases with the rise in the Jeffrey parameter. Hence, the Jeffrey parameter tends to promote the onset of RTI in stratified plasma fluid for both cases. However, it is visualised from the curves in Figs. 7 and 8 that the value of k_{max} gets decreased in the simultaneous presence of quantum pressure and FLR corrections.

Figure 8 illustrates the effect of the Jeffrey parameter on the growth rate of RTI in the presence of quantum pressure and the absence of FLR correction. The curves indicate that an increase in the Jeffrey parameter results in a higher amplitude of the RTI growth rate under the influence of quantum pressure. It is noteworthy to observe from the curves that k_{max} is not attained in the absence of FLR corrections.

Figures 9 and 10 depict the influence of kinematic viscosity on the growth rate of RTI, with and without the inclusion of the Jeffrey parameter, respectively. The plots reveal that kinematic viscosity reduces the instability region in both cases. However, k_{max} is higher for a non-Newtonian fluid than for a Newtonian

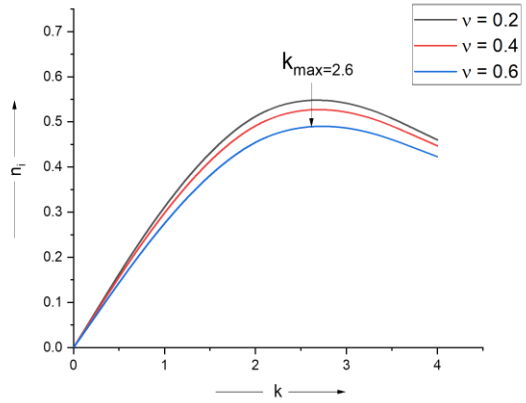

Fig. 9. Impact of kinematic viscosity (ν) on the growth rate of RTI (n_i) against wave number (k), with Jeffrey parameter.

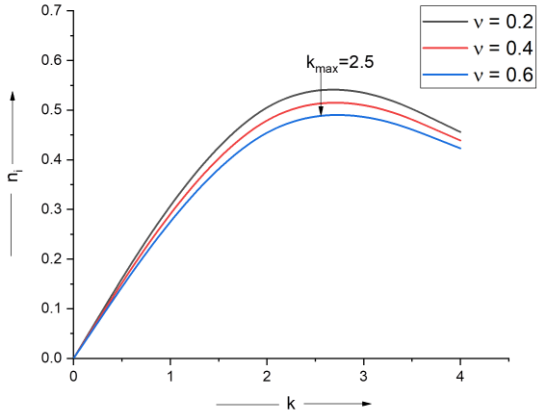

Fig. 10. Impact of the kinematic viscosity (ν) on the growth rate of RTI (n_i) against the wave number (k) in the absence of Jeffrey parameter.

fluid in the present case. These results are in strong agreement with the findings reported by various authors [18−23].

5. Conclusions

The combined effects of quantum pressure and FLR corrections on the RTI in a laminar Jeffrey model plasma fluid are investigated. An explicit dispersion relation for the RTI growth rate is derived, highlighting its dependence on various physical parameters.

- The classical Rayleigh-Taylor instability undergoes significant modification with the inclusion of finite Larmor radius corrections and quantum pressure, resulting in enhanced stability and effective suppression of Rayleigh-Taylor instability in the plasma fluid system.
- The Jeffrey parameter has a destabilising effect on the Rayleigh-Taylor instability of stratified plasma fluid.
- The viscosity of the plasma fluid enhances the stabilisation of the Rayleigh-Taylor instability configuration under the influence of finite Larmor radius corrections and quantum pressure, regardless of the presence of the Jeffrey parameter.
- An important facet of the present study is the demonstration that quantum pressure and finite Larmor radius corrections play a crucial role in various non-Newtonian astrophysical systems, particularly in inertial confinement fusion capsules and white dwarfs.
- The findings offer valuable insights into the non-Newtonian behaviour of astrophysical systems characterised by low temperatures and high densities, enhancing our understanding of their underlying dynamics.

Examining the effects of compressibility, magnetic shear and temperature gradients on the role of finite Larmor radius in the onset of Rayleigh-Taylor instability in stratified magnetised Jeffrey plasma could offer a deeper understanding of the interplay between kinetic effects and macroscopic plasma parameters, thereby improving stability predictions in both astrophysical and laboratory settings.

References

[1] Chandrasekhar, S. (1961). *Hydrodynamic and hydromagnetic stability*. Oxford University Press, Oxford.

[2] Goldston, R.J., & Rutherford, P.H. (1997). *Introduction to plasma physics*. Institute of Physics, London.

[3] Jung, Y.-D. (2001). Quantum-mechanical effects on electron–electron scattering in dense high-temperature plasmas. *Physics of Plasmas*, 8, 3842–3844. doi: 10.1063/1.1386430

[4] Gardner, C.L. (1994). The quantum hydrodynamic model for semiconductor devices. *SIAM Journal on Applied Mathematics*, 54(2), 409–427. https://www.jstor.org/stable/2102225

[5] Haas, F. (2005). A magnetohydrodynamic model for quantum plasma. *Physics of Plasmas*, 12, 062117. doi: 10.1063/1.1939947

[6] Zaitseva, E., Levashenko, V., & Matiaško, K. (2008). Decomposition and estimation of multi-state systems by dynamic reliability indices. *Journal of KONBiN*, 4(1), 53–361. doi: 10.2478/v10040-008-0026-6

[7] Bychkov, V., Marklund, M., & Modestov, M. (2008). The Rayleigh-Taylor instability and internal waves in quantum plasmas. *Physics Letters A*, 372(17), 3042–3045. doi:10.1016/j.physleta.2007.12.065

[8] Sharma, V., Kumari, R., Gupta, S., & Shyam, R. (2017). Stability of stratified viscoelastic Walters' (model B') fluid/plasma in the presence of quantum pressure. *Research Journal of Science and Technology*, 9(1), 201–206. doi: 10.5958/2349-2988.2017.00034.1

[9] Hoshoudy, G.A. (2011). Rayleigh-Taylor instability in quantum magnetized viscous plasma. *Plasma Physics Reports*, 37, 775–784. doi: 10.1134/S1063780X11080046

[10] Hoshoudy, G.A. (2012). External magnetic field effects on the Rayleigh-Taylor instability in an inhomogeneous rotating quantum plasma. *Journal of Modern Physics*, 3, 1792–1801. doi: 10.4236/jmp.2012.311224

[11] Hoshoudy, G.A. (2014). Rayleigh-Taylor instability in magnetized plasma. *World Journal of Mechanics*, 4, 260–272. doi: 10.4236/wjm.2014.48027

[12] Hoshoudy, G.A., & Awasthi, M.K. (2020). Compressibility effects on the Kelvin-Helmholtz and Rayleigh-Taylor instabilities between two immiscible fluids flowing through a porous medium. *The European Physical Journal Plus*, 135, 169. doi: 10.1140/epjp/s13360-020-00160-x

[13] Hoshoudy, G.A., & Prajapati, R.P. (2016). Quantum effects on the Rayleigh–Taylor instability of stratified plasma in the presence of suspended particles. *Pramana – Journal of Physics*, 87, 99. doi: 10.1007/s12043-016-1297-4

[14] Sharma, V., & Gupta, U. (2010). Stability of stratified elasto-viscous Walters' (model B') fluid in the presence of horizontal magnetic field and rotation. *Studia Geotechnika et Mechanica*, 32(2), 41–54.

[15] Dolai, B., & Prajapati, R.P. (2018). The rotating Rayleigh-Taylor instability in a strongly coupled dusty plasma. *Physics of Plasmas*, 25(8), 083708. doi:10.1063/1.5041088

[16] Rosenbluth, M.N., Krall, N.A., & Rostoker, N. (1961). *Finite Larmor radius stabilization of 'weakly' unstable confined plasmas*. *Nuclear Fusion, Supplement*, GA-2371.

[17] Roberts, K.V., & Taylor, J.B. (1962) Magnetohydrodynamic equations for finite Larmor radius. *Physical Review Letters*, 8, 197. doi: 10.1103/PhysRevLett.8.197

[18] Jukes, J.D. (1964). Gravitational resistive instabilities in plasma with finite Larmor radius. *Physics of Fluids*, 7(1), 52–58. doi: 10.1063/1.1711054

[19] Surindar, S., & Harikrishan, H. (1966). Magnetic viscosity and the stability of superposed fluids in a magnetic field. *Nuclear Fusion*, 6(1), 6. doi: 10.1088/0029-5515/6/1/002

[20] Sanghvi, R.K., & Chhajlani, R.K. (1987). Finite Larmor-radius effects on Rayleigh-Taylor instability of a dusty magnetized plasma. *Astrophysics and Space Science*, 132, 57–64. doi: 10.1007/BF00637781

[21] Sharma, P.K., & Chhajlani, R.K. (1998). Effect of rotation on the Rayleigh-Taylor instability of two superposed magnetized conducting plasma. *Physics of Plasmas*, 5(6), 2203–2209. doi: 10.1063/1.872893

[22] Sayed, A.H. (2010). *Fundamentals of adaptive filtering*. Wiley India, Delhi.

[23] Tiwari, A., Argal, S., Khan, N., & Sharma, P.K. (2018). Quantum and FLR effects on the Rayleigh Taylor instability of stratified plasmas. *Physics of Plasmas*, 25(1), 012109. doi: 10.1063/5.0057762

[24] Sun, Y.B., Gou, J.N., & Wang, C. (2021). Combined effects of viscosity and a vertical magnetic field on Rayleigh-Taylor instability. *Physics of Plasmas*, 28(9), 092707. doi: 10.1063/5.0057762

[25] Joseph, D.D., & Preziosi, L. (1989). Heat waves. *Reviews of Modern Physics*, 61(1), 41–73. doi: 10.1103/RevModPhys.61.41

[26] Yadav, D. (2021). Influence of anisotropy on the Jeffrey fluid convection in a horizontal rotary porous layer. *Heat Transfer*, 50(5), 4595–4606. doi: 10.1002/htj.22090

[27] Yadav, D. (2022). Effect of electric field on the onset of Jeffery fluid convection in a heat-generating porous medium layer. *Pramana – Journal of Physics*, 96, 19 doi: 10.1007/s12043-021-02242-6

[28] Yadav, D. (2022). Thermal non-equilibrium effects on the instability mechanism in a non-Newtonian Jeffrey fluid saturated porous layer. *Journal of Porous Media*, 25(2), 1–12. doi: 10.1615/JPorMedia.2021038392

[29] Gautam, P.K., Rana, G.C., & Saxena, H. (2020). Stationary convection in the electrohydrodynamic thermal instability of Jeffrey nanofluid layer saturating a porous medium: free-free, rigid-free, and rigid-rigid boundary conditions. *Journal of Porous Media*, 23(11), 1043–1063. doi: 10.1615/JPorMedia.2020035061

[30] Sharma, V., Thakur, A., Devi, J., & Rana, G.C. (2023). Rayleigh-Taylor instability of superposed dusty Jeffrey fluids through porous medium with interfacial surface tension. *Acta Physica Polonica A*, 143(3), 238–245. doi: 10.12693/APhysPolA.143.238

[31] Yadav, D., Mohamad, A.A., & Awasthi, M.K. (2021). The Horton-Rogers-Lapwood problem in a Jeffrey fluid influenced by a vertical magnetic field. *Proceedings of the Institution of Mechanical Engineers, Part E: Journal of Process Mechanical Engineering*. 235(6), 2119–2128. doi: 10.1177/09544089211031108

[32] Yadav, D., Al-Balushi, S., Awasthi, M.K., Al-Hadi, T., Al-Abri, R., Al-Wahaibi, J., Al-Nasseri, F., Al-Siyabi, S., Ragoju, R., & Bhattacharyya, K. (2023). Convective flow of ethylene glycol-silver Jeffery nanofluid in a Hele-Shaw cell with an influence of external magnetic field. *Asia-Pacific Journal of Chemical Engineering*, 18(3), 2884. doi: 10.1002/apj.2884

[33] Prajapati, R.P. (2016). Rayleigh-Taylor instability in non-uniform magnetized rotating strongly coupled viscoelastic fluid. *Physics of Plasmas*, 23(2), 022106. doi: 10.1063/1.4941593

[34] Garai, S., Ghose-Choudhury, A., & Guha, P. (2020). Rayleigh Taylor like instability in presence of shear velocity in a strongly coupled quantum plasma. *Physica Scripta*, 95(10), 105605. doi: 10.1088/1402-4896/abb697

[35] Dey, D. (2018). Dusty Jeffrey fluid flow in a rotating system with volume fraction and Hall effect: An analytical approach. *Advances in Modelling and Analysis A*, 55(2), 70–75. doi: 10.18280/ama_a.550205

[36] Garai, S., Banerjee, D., Janaki, M.S., & Chakrabarti, N. (2015) Stabilization of Rayleigh-Taylor instability in a non-Newtonian incompressible complex plasma. *Physics of Plasmas*, 22, 033702. doi: 10.1063/1.4916126

[37] Adak, A., Ghosh, S., & Chakrabarti, N. (2024). Rayleigh-Taylor instability in an equal mass plasma. *Physics of Plasmas*, 21, 09120. doi: 10.1063/1.4896714

[38] Das, A., Dharodi, V., & Tiwari, S. (2014). Collective dynamics in strongly coupled dusty plasma medium. *Journal of Plasma Physics*, 80(6), 855–861. doi: 10.1017/S0022377814000506

[39] Dharodi, V.S., & Das, A. (2021). A numerical study of gravity-driven instability in strongly coupled dusty plasma. Part 1. Rayleigh-Taylor instability and buoyancy-driven instability. *Journal of Plasma Physics* 87(2), 905870216. doi: 10.1017/S0022377821000349

[40] Dharodi, V.S. (2021). A numerical study of gravity-driven instability in strongly coupled dusty plasma. Part 2. Hetero-interactions between a rising bubble and a falling droplet. *Journal of Plasma Physics*, 87(4), 905870402. doi: 10.1017/ S0022377821000684

[41] Dharodi, V.S. (2024). A numerical study of gravity-driven instability in strongly coupled dusty plasma. Part 3. Homo-interaction between a pair of rising/falling bubbles/droplets. *Journal of Plasma Physics*, 90(4), 905900408. doi: 10.1017/S0022377824001144